

A Theoretical Framework for Quantitative Analysis of the Molecular Basis of Costimulation

Andreas Jansson,^{*†} Eleanor Barnes,[‡] Paul Klenerman,[‡] Mikael Harlén,^{*} Poul Sørensen,[¶] Simon J. Davis,^{1§} and Patric Nilsson^{*}

We present a theoretical framework for simulating the synaptic accumulation of the costimulatory molecules CD28, CTLA-4, B7-1, and B7-2, based on a system of mean-field, ordinary differential equations, and rigorous biophysical and expression data. The simulations show that binding affinity, stoichiometric properties, expression levels, and, in particular, competition effects all profoundly influence complex formation at cellular interfaces. B7-2 engages 33-fold more CD28 than CTLA-4 at the synapse in contrast to B7-1, which ligates ~7-fold more CTLA-4 than CD28. Although B7-1 completely dominates interactions with CTLA-4, forming linear arrays of 7-18 receptor-ligand pairs, CTLA-4 is fully engaged by B7-2 when B7-1 is absent. Additional simulations reveal the sensitivity of CD28 interactions to modeled transport processes. The results support the concept that B7-2 and B7-1 are the dominant ligands of CD28 and CTLA-4, respectively, and indicate that the inability of B7-2 to recruit CTLA-4 to the synapse cannot be due to the differential binding properties of B7-1 and B7-2 only. We discuss the apparent redundancy of B7-1 in the context of a potentially dynamic synaptic microenvironment, and in light of functions other than the direct enhancement of T cell inhibition by CTLA-4. *The Journal of Immunology*, 2005, 175: 1575–1585.

Mathematical modeling is making significant inroads toward unraveling the complexity of leukocyte recognition and activation (reviewed by Chakraborty et al. (1) and Goldstein et al. (2)). The “kinetic proofreading” model, which may explain how T cells discriminate between ligands on the basis of TCR/peptide-MHC (pMHC)² interaction half-lives (3), has been assimilated into most theories of TCR function and extended to aggregating receptors and receptor systems dependent on extrinsic kinases (4). Related models have implied that the balance between encounter rates and the TCR/pMHC bond lifetime, i.e., between serial engagement (5) and kinetic proofreading, determines the range of k_{off} values over which pMHC complexes are active (6). Simulations have also revealed how the interplay of TCR/pMHC and LFA-1/ICAM-1 complex topologies and the mechanical properties of cytoskeleton-attached cell membranes could engender an intrinsic tendency for the receptor segregation characteristic of the mature immunological synapse (e.g., see Refs. 7–11). Finally, in silico approaches have been used to support the concept that TCR signaling and degradation balance one another at the synapse (12).

The immunological synapse is characterized by a ring of engaged large adhesion molecules (i.e., the peripheral (p)-supramolecular activation cluster (SMAC)) surrounding a region of clustered, ligand-bound TCRs, referred to as the central SMAC (c-

SMAC) (13, 14). Although its precise function is uncertain (15), it seems clear, at the very least, that the synapse creates a microenvironment favoring the interactions of cell-cell recognition proteins. The best evidence for this emerged from an analysis of the role of B7-1-CD28 interactions in synapse formation, which showed that the rate of synapse formation and the degree of TCR accumulation in the central cluster are each unaffected by the presence of B7-1, and that CD28-B7-1 interactions remain undetectable until close contacts are induced by other topologically similar molecules, such as CD2 (16). As such, synaptic protein interactions are uniquely well-suited to in silico simulation because their formation within a fully formed, stable synapse implies that membrane approximation and mechanical stress or unbinding forces do not have to be explicitly modeled. The costimulatory system is also appealing as a subject for simulation because the structures, stoichiometries, and affinities of the interactions of these proteins are among the best understood for any receptor-ligand signaling system.

CD28 and CTLA-4 are related type I membrane glycoproteins expressed at the T cell surface as disulphide-linked homodimers that generate coactivating and inhibitory signals, respectively (17, 18). CD28 is monovalent and constitutively expressed at relatively high levels. In contrast, very small amounts of bivalent, CTLA-4 homodimers are delivered from intracellular stores directly into the synapse relatively late in T cell activation (19). CD28 and CTLA-4 bind shared ligands, B7-1 and B7-2, which were initially thought to have comparable structures and affinities for their receptors and, therefore, overlapping functions. However, Collins et al. (20) have identified large affinity and stoichiometric differences between B7-1 and B7-2. In solution, B7-2 binds CD28 and CTLA-4 considerably more weakly than B7-1 whereas, relative to its CTLA-4-binding affinity, B7-2 binds CD28 2- to 3-fold more effectively than B7-1; moreover, unlike B7-1, B7-2 does not self-associate (Fig. 1A; Refs. 20–22). These observations suggest that, when coexpressed at the cell surface, B7-1 will markedly favor CTLA-4 over CD28 engagement, whereas B7-2 will exhibit much less bias toward CTLA-4. The possibility that costimulatory signaling by B7-2 will be less compromised by coincident inhibitory signals from CTLA-4 than that by B7-1 provides an explanation for the

*Computational Biology, School of Life Sciences, University of Skövde, Skövde, Sweden; [†]School of Biotechnology and Biomolecular Sciences, University of New South Wales, Sydney, New South Wales, Australia; [‡]Nuffield Department of Clinical Medicine, Peter Medawar Building for Pathogen Research, University of Oxford, and [§]Nuffield Department of Clinical Medicine, University of Oxford, John Radcliffe Hospital, Oxford, United Kingdom; and [¶]LEO Pharma, Ballerup, Denmark

Received for publication November 1, 2004. Accepted for publication May 16, 2005.

The costs of publication of this article were defrayed in part by the payment of page charges. This article must therefore be hereby marked *advertisement* in accordance with 18 U.S.C. Section 1734 solely to indicate this fact.

¹ Address correspondence and reprint requests to Prof. Simon J. Davis, Medical Research Council Human Immunology Unit and Nuffield Department of Clinical Medicine, University of Oxford, John Radcliffe Hospital, Headington, Oxford OX3 9DU, U.K. E-mail address: simon.davis@clinical-medicine.oxford.ac.uk

² Abbreviations used in this paper: pMHC, peptide MHC; SMAC, supramolecular activation cluster; p-SMAC, peripheral-SMAC; c-SMAC, central SMAC; DC, dendritic cell; iDC, immature DC; mDC, mature DC.

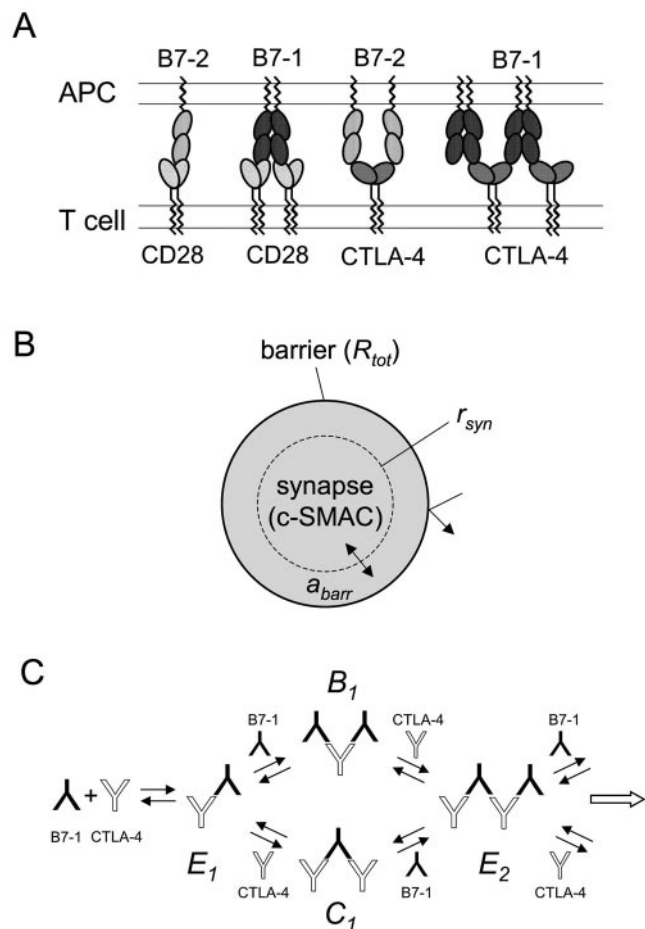


FIGURE 1. A, The various interactions of costimulatory molecules. Whereas CD28 and B7-2 form monovalent complexes, both CD28 and B7-1, and CTLA-4 and B7-2, form bivalent complexes. The bivalency of both CTLA-4 and B7-1 allows the formation of multivalent complexes. B, Assumptions incorporated into the barrier-diffusion/active transport model. It is assumed that the c-SMAC of the synapse forms within a membrane “corral” consisting of a region of the cell surface bounded by a membrane barrier (shaded area; reviewed by Vereb et al. (25)). Molecules located in the area (a_{barr}) between the edge of the synapse (r_{syn}) and the membrane barrier (R_{tot}) may diffuse into the synapse and vice versa. Molecules outside the corral cannot move beyond the barrier into the vicinity of the synapse unless actively transported there. Active transport is modeled by placing a certain fraction of molecules within the corral. C, Scheme depicting the sequential formation of multivalent complexes by B7-1 and CTLA-4.

distinct effects on T cell responses of B7-1 vs B7-2, as revealed by Ab blockade experiments (20). The affinity and stoichiometric differences described by Collins et al. (20) have also been proposed to account for the observations that CD28 is apparently recruited to the synapse by B7-2 only, whereas B7-1 exclusively recruits CTLA-4 (23).

These predictions can be tested in a relatively straightforward manner using simulations of synaptic interactions based on mean-field, ordinary differential equations and stoichiometric and affinity measurements, diffusion rates and expression data. We generate such equations and use them to illuminate the relationship between the properties of protein interactions measured in solution and their likely features at intercellular junctions. The simulations show that the processes governing the accumulation of costimulatory receptors may be more complex than anticipated, because affinity and stoichiometric differences are insufficient to account for the observed behavior (23) of CTLA-4 at the synapse. Unexpectedly, our

simulations also suggest that B7-1 is largely redundant within this system, insofar as it is currently understood. We discuss these observations in the context of a potentially dynamic synaptic microenvironment, and in light of other possible functions of B7-1, rather than the direct enhancement of T cell inhibition by CTLA-4. Our work emphasizes the usefulness of quantitative methods for dissecting complex immunological phenomena.

Materials and Methods

Equations

We use a simple two-compartment model, similar to that used previously (24), to simulate CD28 and CTLA-4 complex formation at synapses between a dendritic cell (DC) and a Th cell. The two compartments consist of the c-SMAC of the synapse and the region outside it; for the purposes of this study, synapse and c-SMAC are used synonymously. CD28, B7-1, and B7-2 are initially unligated and uniformly distributed over the surface. CTLA-4, however, is stored intracellularly and is injected into the synapse upon activation (19). Complex formation will deplete the pool of unbound molecules, resulting in the recruitment of additional molecules from the outer compartment. Recruitment of molecules into the synapse is therefore a passive, diffusion-driven process, which maintains equal densities of unbound molecules in the areas inside and outside the synapse.

We use two different approaches to impose restrictions on the mobility of the molecules. The first allows only a fraction of the molecules to diffuse freely at the cell surface (the “free-diffusion” model). The second model, which we refer to as the “barrier-diffusion/active transport” model, relies on the observation that the movement of surface molecules appears to be restricted to short distances by “corrals” within the membrane, as revealed by studies of wild-type class I MHC molecules, which exhibit a barrier-free path of ~ 600 nm (25). This distance is somewhat larger for mutant class I lacking the cytoplasmic domain, suggesting that the effect is due to physical barriers located close to the inner leaflet of the membrane, rather than the presence of membrane “rafts” (25). To simulate the effects of such barriers, we assume 1) that the c-SMAC of the synapse forms within one of these corrals (i.e., the shaded area in Fig. 1B) and (ii) that only the molecules present within the corral are able to reach the synapse. In the simulations, the distance between the barrier at the edge of the corral and the synapse is taken to be $0.5 \mu\text{m}$. To simulate the effects of active transport under such conditions, we place differing fractions of molecules within the corral at the start of our simulations. The recruitment of molecules into the synapse thereafter is diffusion-driven, as in the free-diffusion model. For the barrier-diffusion/active transport model the molecules are all assumed to be fully mobile.

All numerical simulation procedures were programmed in MATLAB (The Math Works). A finite difference method was used to integrate the system of coupled nonlinear ordinary differential equations. Because the system is stiff, i.e., it has a large variation in its response, a multistep method of variable ordering was used. The variables used are those listed in Table I; parameters are defined in Tables II-V.

Molecule partitioning into the synapse

The free-diffusion model. The free-diffusion model assumes: 1) that various fractions of the molecules are mobile and immobile (16) and that only mobile molecules are able to diffuse into the synapse; immobile molecules outside the synapse are ignored because they will not participate in the interactions within the synapse; 2) that the immobile molecules located inside the synapse at the initial cell-to-cell contact are assumed to remain there, and to be capable of binding ligands; and 3) that injected CTLA-4 molecules remain within the synapse (see *Intracellular and surface levels of CTLA-4*). The mobile molecules are assumed to diffuse freely on a perfect sphere (the cell surface) to reach the synapse. The rate constant, k_{in} , for molecules diffusing into the synapse is estimated according to the method of Agrawal and Linderman (24):

$$k_{in} = \frac{D}{R^2} \left(\frac{1 + \cos \theta}{2 \ln(2(1 - \cos \theta)^{-1}) - (1 + \cos \theta)} \right) \quad (1.1)$$

using an appropriate diffusion coefficient D , cell radius R , radius of contact area r_{syn} , and angle defining the boundary of the synapse $\theta = r_{syn}/R$. This method ensures that the unbound molecules are distributed equally in the absence of binding. The diffusion rate out of the synapse, k_{out} , is estimated by:

$$k_{out} = k_{in} \left(\frac{a_{outside}}{a_{syn}} \right) \quad (1.2)$$

Table I. *Definition of variables*

Name	Definition	Units
$T_{CD28,out}$	Amount of mobile CD28 outside the synapse	Number
$T_{CD28,syn}$	Density of free CD28 inside the synapse	Number/ μm^2
$T_{CTLA,Barr}$	Density of mobile surface CTLA-4 outside the synapse in the barrier-diffusion/active transport model	Number/ μm^2
$T_{CTLA,int}$	Amount of intracellular CTLA-4	Number
$T_{CTLA,syn}$	Density of free CTLA-4 inside the synapse	Number/ μm^2
$D_{B71,out}$	Amount of mobile B7-1 outside the synapse	Number
$D_{B71,syn}$	Density of free B7-1 inside the synapse	Number/ μm^2
$D_{B72,out}$	Amount of mobile B7-2 outside the synapse	Number
$D_{B72,syn}$	Density of free B7-2 inside the synapse	Number/ μm^2
$C_{CD28:B72}$	Density of CD28/B7-2 complexes	Number/ μm^2
$C_{CD28:B71}$	Density of monovalent CD28/B7-1 complexes	Number/ μm^2
$C_{(CD28)2:B71}$	Density of bivalent CD28/B7-1 complexes	Number/ μm^2
$C_{CTLA:B72}$	Density of monovalent CTLA-4/B7-2 complexes	Number/ μm^2
$C_{CTLA:(B72)2}$	Density of bivalent CTLA-4/B7-2 complexes	Number/ μm^2
B_k	Density of multivalent CTLA-4/B7-1 complexes with k bound CTLA-4	Number/ μm^2
C_k	Density of multivalent CTLA-4/B7-1 complexes with $k + 1$ bound CTLA-4	Number/ μm^2
E_k	Density of CTLA-4/B7-1 complexes with k bound CTLA-4	Number/ μm^2

where a_{syn} is the area of the synapse and $a_{outside}$ is the area of the region outside the synapse.

The barrier-diffusion/active transport model. A second model assumes: 1) that all molecules are mobile but the mobility is restricted by corrals in the cell membrane (25); 2) that the c-SMAC of the synapse forms within one of these corrals; 3) that the average barrier-free path extends to 0.5 μm beyond the edge of the synapse to the edge of the corral and that molecules located $>0.5 \mu\text{m}$ from the synapse, i.e., outside the corral, are ignored because they cannot reach the synapse; and 4) that the diffusion of CTLA-4 injected into the synapse is limited by a barrier 0.5 μm from the synapse edge. Active transport is simulated by assuming that certain fractions of the molecules have been transported to the corral and are thereafter constrained by the barrier 0.5 μm from the synapse. It is assumed that the synapse is the disc $x^2 + y^2 \leq r_{syn}^2$ and that the molecules stay within the planar disc $x^2 + y^2 \leq R_{tot}^2$ representing the corral (Fig. 1B). Molecules within the region $r_{syn}^2 \leq x^2 + y^2 \leq R_{tot}^2$ diffuse into the synapse at rate k_{in} , estimated according to the method of Szabo et al. (26), which is based on an analysis of the average time required for absorption, $\tau = \tau(x, y)$, of a particle starting at the point (x, y) . The relation between the diffusion rate and the average time required for absorption is given by:

$$\frac{1}{k_{in}} = \iint_{r_{syn}^2 \leq x^2 + y^2 \leq R_{tot}^2} \tau p \, dx \, dy \quad (2.1)$$

where p is the distribution of starting points, which is assumed to be an equal distribution, i.e.,

$$p = 1 / \iint_{r_{syn}^2 \leq x^2 + y^2 \leq R_{tot}^2} dx \, dy = 1/\pi(R_{tot}^2 - r_{syn}^2). \quad (2.2)$$

The average time required for absorption fulfils the adjointed diffusion equation, i.e.,

$$D\Delta\tau = -1 \quad (2.3)$$

where Δ denotes the Laplacian and D denotes the diffusion coefficient. Changing into polar coordinates and stating the appropriate boundary conditions implies:

$$\begin{cases} \frac{1}{r} \frac{d}{dr} rD \frac{d}{dr} \tau = -1, & r_{syn} < r < R_{tot}, \\ \tau(r_{syn}) = 0, \\ \frac{d\tau}{dr}(R_{tot}) = 0. \end{cases} \quad (2.4)$$

The boundary condition at $r = r_{syn}$ is the absorption property at the synapse boundary and the boundary condition at $r = R_{tot}$ is the reflection property at the barrier. Solving this differential equation, subject to the stated boundary conditions, is straightforward:

$$\tau(r) = \frac{1}{D} \left(\frac{r_{syn}^2 - r^2}{4} + \frac{R_{tot}}{2} (\ln r - \ln r_{syn}) \right). \quad (2.5)$$

Finally, to obtain k_{in} we combine this with equations 2.1 and 2.2 to obtain:

$$\begin{aligned} \frac{1}{k_{in}} &= \iint_{r_{syn}^2 \leq x^2 + y^2 \leq R_{tot}^2} \tau(x, y) p(x, y) \, dx \, dy \\ &= 2\pi \int_{r_{syn}}^{R_{tot}} \tau(r) p(r) r \, dr \\ &= \frac{1}{8D(R_{tot}^2 - r_{syn}^2)} \\ &= (4r_{syn}^2 R_{tot}^2 - 3R_{tot}^4 + 4R_{tot}^4 \ln R_{tot} - 4R_{tot}^4 \ln r_{syn} - r_{syn}^4). \end{aligned} \quad (2.6)$$

Table II. *Parameters used for calculating the diffusion rates*

Name	Definition	Value	Ref.
R_{aTcell}	Radius of an activated Th cell	6.0 μm	43
R_{nTcell}	Radius of a naive Th cell	3.0 μm	44
R_{DC}	Radius of a DC	10 μm	45
R_{tot}	Radius of total diffusion area in the barrier-diffusion/active transport model	2.5 μm	
r_{syn}	Radius of synapse (c-SMAC)	2.0 μm	14
a_{syn}	Area of synapse	12.6 μm^2	14
a_{Barr}	Barrier area outside the synapse ($r_{syn}^2 \leq x^2 + y^2 \leq R_{tot}^2$)	7.07 μm^2	
D	Diffusion coefficient	0.1 $\mu\text{m}^2 \text{s}^{-1}$	30, 31

Table III. Rate constants used in the free-diffusion model (i) and in the barrier-diffusion/active transport model (ii)

Name	Definition	(i)	(ii)	Units	Ref.
κ_{28}	Rate constant for CD28 diffusing out from synapse (naive/activated)	$5.9 \times 10^{-2}{}^a$ $3.6 \times 10^{-2}{}^a$	$0.60{}^a$	s^{-1}	24, 26
γ_{28}	Rate constant for CD28 diffusing into synapse (naive/activated)	$7.4 \times 10^{-3}{}^a$ $1.0 \times 10^{-3}{}^a$	$1.07{}^a$	s^{-1}	24, 26
λ	Injection rate of CTLA-4	$7.7 \times 10^{-3}{}^b$	$7.7 \times 10^{-3}{}^b$	s^{-1}	19
κ_{Barr}	Rate constant for CTLA-4 diffusing out from synapse		$0.60{}^a$	s^{-1}	26
γ_{Barr}	Rate constant for CTLA-4 diffusing into synapse		$1.07{}^a$	s^{-1}	26
κ_{DC}	Rate constant for molecules on DC diffusing out from synapse	$2.7 \times 10^{-2}{}^a$	$0.60{}^a$	s^{-1}	24, 26
γ_{DC}	Rate constant for molecules on DC diffusing into synapse	$2.7 \times 10^{-4}{}^a$	$1.07{}^a$	s^{-1}	24, 26

^a The calculated diffusion rates are average rates for diffusion in and out of the synapse.

^b Injection rate for CTLA-4 was estimated according to the work of Egen and Allison (19).

Similar calculations may be used to obtain diffusion rates out of the synapse. However, to ensure that the unbound molecules are distributed equally in the absence of binding, k_{out} is calculated as given in equation 1.2.

Complex formation

Three-dimensional rate constants (i.e., measured in solution) for each of the protein interactions (20), were converted to two-dimensional rate constants using the following formula (27):

$$2D K_d = 3D K_d \cdot \sigma$$

where σ is the confinement region (3 nm; Ref. 16) to which the ligand-binding sites of the two receptors are restricted. Equations simulating-complex formation consist of terms accounting for the association (α) between molecules on the T cell (T) and the dendritic cell (D) as well as the dissociation (δ) of the complexes (C). Allowance is given for the distinct binding kinetics along with the bivalency of CTLA-4 and B7-1 and the monovalency of B7-2 and CD28 (Fig. 1A). The rate of the monovalent interaction between B7-2 and CD28 is given by:

$$\frac{dC_{\text{CD28:B72}}}{dt} = \alpha_1 T_{\text{CD28,syn}} D_{\text{B72,syn}} - \delta_1 C_{\text{CD28:B72}}. \quad (3.1)$$

Unbound CD28 ($T_{\text{CD28,syn}}$) and B7-2 ($D_{\text{B72,syn}}$) molecules inside the synapse interact with an association rate α_j , giving CD28/B7-2 complexes ($C_{\text{CD28:B72}}$). These complexes dissociate at rate δ_j . Equations that describe the rates of monovalent and bivalent interactions between B7-1 and CD28 are as follows:

$$\begin{aligned} \frac{dC_{\text{CD28:B71}}}{dt} &= \alpha_2 T_{\text{CD28,syn}} D_{\text{B71,syn}} - \delta_2 C_{\text{CD28:B71}} \\ &\quad - \alpha_{22} T_{\text{CD28,syn}} C_{\text{CD28:B71}} + \delta_{22} C_{(\text{CD28})2:\text{B71}} \end{aligned} \quad (3.2)$$

$$\frac{dC_{(\text{CD28})2:\text{B71}}}{dt} = \alpha_{22} T_{\text{CD28,syn}} C_{\text{CD28:B71}} - \delta_{22} C_{(\text{CD28})2:\text{B71}}. \quad (3.3)$$

CD28 associates with B7-1 at rate α_2 , generating CD28/B7-1 complexes ($C_{\text{CD28:B71}}$) that may either dissociate at rate δ_2 or associate with a second CD28 molecule at rate α_{22} . The bivalently bound B7-1 molecules ($C_{(\text{CD28})2:\text{B71}}$) dissociate at rate δ_{22} . CTLA-4/B7-2 interactions are described in a manner analogous to that for CD28/B7-1 interactions, and are therefore given by:

$$\begin{aligned} \frac{dC_{\text{CTLA4:B72}}}{dt} &= \alpha_3 T_{\text{CTLA4,syn}} D_{\text{B72,syn}} - \delta_3 C_{\text{CTLA4:B72}} \\ &\quad - \alpha_{33} C_{\text{CTLA4:B72}} D_{\text{B72,syn}} + \delta_{33} C_{\text{CTLA4:(B72)2}} \end{aligned} \quad (3.4)$$

$$\frac{dC_{\text{CTLA4:(B72)2}}}{dt} = \alpha_{33} C_{\text{CTLA4:B72}} D_{\text{B72,syn}} - \delta_{33} C_{\text{CTLA4:(B72)2}}. \quad (3.5)$$

The interaction of B7-1 with CTLA-4 can generate multivalent complexes because both molecules are bivalent (Fig. 1C). The free, unbound B7-1 and CTLA-4 inside the synapse can form monovalent complexes, given by:

$$\begin{aligned} \frac{dE_1}{dt} &= \alpha_4 T_{\text{CTLA4,syn}} D_{\text{B71,syn}} - \delta_4 E_1 - \alpha_{44} T_{\text{CTLA4,syn}} E_1 \\ &\quad - \alpha_{44} D_{\text{B71,syn}} E_1 + \delta_{44} B_1 + \delta_{44} C_1. \end{aligned} \quad (3.6)$$

CTLA-4 associates with B7-1 at rate α_4 generating complex E_1 . The E_1 complex may dissociate at rate δ_4 , or associate with either B7-1 or CTLA-4 at rate α_{44} , which results in B_1 and C_1 complexes, respectively. The dissociation of B_1 and C_1 complexes results in E_1 complexes and in unbound B7-1 and CTLA-4 molecules, respectively, at rate δ_{44} . The multivalent binding of B7-1 with CTLA-4 can result in the formation of three types of complexes, each of arbitrary length. For each positive

Table IV. Association and dissociation rates

Name	Definition	Rate	Ref.
α_1	Association of CD28 and B7-2	$0.77 \mu\text{m}^2 \text{s}^{-1}$	20, 29
α_2	Association of CD28 and B7-1	$0.22 \mu\text{m}^2 \text{s}^{-1}$	20, 29
α_3	Association of CTLA-4 and B7-2	$1.09 \mu\text{m}^2 \text{s}^{-1}$	20, 29
α_4	Association of CTLA-4 and B7-1	$1.19 \mu\text{m}^2 \text{s}^{-1}$	20, 29
α_{22}	Bivalent association of CD28 and B7-1	$0.22 \mu\text{m}^2 \text{s}^{-1}$	20, 29
α_{33}	Bivalent association of CTLA-4 and B7-2	$0.13 \mu\text{m}^2 \text{s}^{-1}$	20, 29
α_{44}	Multivalent association of CTLA-4 and B7-1	$0.17 \mu\text{m}^2 \text{s}^{-1}$	20, 29
δ_1	Dissociation of CD28/B7-2	28s^{-1}	20, 29
δ_2	Dissociation of CD28/B7-1	1.6s^{-1}	20, 29
δ_3	Dissociation of CTLA-4/B7-2	5.1s^{-1}	20, 29
δ_4	Dissociation of CTLA-4/B7-1	0.43s^{-1}	20, 29
δ_{22}	Dissociation of bivalent CD28/B7-1	1.6s^{-1}	20, 29
δ_{33}	Dissociation of bivalent CTLA-4/B7-2	0.052s^{-1}	20, 29
δ_{44}	Dissociation of multivalent CTLA-4/B7-1	0.0044s^{-1}	20, 29

integer k , the rates of change are given by the following differential equations:

$$\frac{dB_k}{dt} = -\alpha_{44}T_{CTLA, \text{syn}}B_k - \delta_{44}B_k + \alpha_{44}D_{B71, \text{syn}}E_k + \delta_{44}\frac{E_{k+1}}{2} \quad (3.7)$$

$$\frac{dC_k}{dt} = -\alpha_{44}D_{B71, \text{syn}}C_k - \delta_{44}C_k + \alpha_{44}T_{CTLA, \text{syn}}E_k + \delta_{44}\frac{E_{k+1}}{2} \quad (3.8)$$

$$\begin{aligned} \frac{dE_{k+1}}{dt} = & \alpha_{44}T_{CTLA, \text{syn}}B_k + \alpha_{44}D_{B71, \text{syn}}C_k - \alpha_{44}D_{B71, \text{syn}}E_{k+1} \\ & - \alpha_{44}T_{CTLA, \text{syn}}E_{k+1} - \delta_{44}E_{k+1} + \delta_{44}B_{k+1} + \delta_{44}C_{k+1}. \end{aligned} \quad (3.9)$$

The B_k and C_k complexes may associate with CTLA-4 and B7-1, respectively, at rate α_{44} , which generates E_{k+1} complexes, or they can dissociate into E_k complexes at rate δ_{44} . The E_{k+1} complex may associate with either B7-1 or CTLA-4 to form B_{k+1} and C_{k+1} complexes, respectively, or dissociate into either B_k or C_k complexes. Theoretically, these multivalent interactions may continue until all of the free cell surface molecules are depleted.

Mobile molecules outside the synapse

The number of mobile CD28, B7-1, and B7-2 molecules outside the synapse is estimated based on the total number of molecules (t_{tot} , which is assumed to be constant), their actual mobility (m), the synapse area (a_{syn}), and the density of mobile molecules inside the synapse. The density of mobile molecules inside the synapse is given by the density of unbound molecules ($T_{CD28, \text{syn}}$, $D_{B71, \text{syn}}$, or $D_{B72, \text{syn}}$) and the density of complexes and immobile molecules (i). Thus, the total amounts of mobile CD28, B7-1, and B7-2 outside the synapse ($T_{CD28, \text{out}}$, $D_{B71, \text{out}}$, $D_{B72, \text{out}}$), respectively, are given by:

$$\begin{aligned} T_{CD28, \text{out}} = & t_{CD28, \text{tot}}m_{CD28} - (T_{CD28, \text{syn}} + C_{CD28: B71} \\ & + 2C_{(CD28)2: B71} + C_{CD28: B72} - i_{CD28})a_{\text{syn}}. \end{aligned} \quad (4.1)$$

$$\begin{aligned} D_{B71, \text{out}} = & t_{B71, \text{tot}}m_{B71} - (D_{B71, \text{syn}} + C_{CD28: B71} + C_{(CD28)2: B71} \\ & + \sum_{k=1}^{\infty} B_k(k+1) + \sum_{k=1}^{\infty} C_k k + \sum_{k=1}^{\infty} E_k k - i_{B71})a_{\text{syn}} \end{aligned} \quad (4.2)$$

$$\begin{aligned} D_{B72, \text{out}} = & t_{B72, \text{tot}}m_{B72} - (D_{B72, \text{syn}} + C_{CD28: B72} + C_{CTLA: B72} \\ & + 2C_{CTLA: (B72)2} - i_{B72})a_{\text{syn}}. \end{aligned} \quad (4.3)$$

Intracellular and surface levels of CTLA-4

CTLA-4 is assumed to be stored in intracellular vesicles ($T_{CTLA, \text{int}}$), initially. In the free-diffusion model of CTLA-4/B7 complex formation, CTLA-4 molecules are injected into the synapse in accordance with the findings of Egen and Allison (19) and constrained there, following the observations of Linsley et al. (28); the term, $T_{CTLA, \text{Barr}}$, in equation 4.4 therefore equals zero in this model. Numbers of CTLA-4 complexes are calculated as in equations 4.1–4.3. In simulations without constraints on diffusion, the CTLA-4 is completely ligated and also remains within the synapse (data not shown). The barrier-diffusion/active transport model considers that injected CTLA-4 molecules are free to diffuse out (κ_{Barr}) into the corral, i.e., the area bounded by the barrier $0.5 \mu\text{m}$ beyond the edge of the synapse (a_{Barr}). CTLA-4 molecules within this area, ($T_{CTLA, \text{Barr}}$) may also diffuse back into the synapse at rate γ_{Barr} . The number of intracellular ($T_{CTLA, \text{int}}$) and surface ($T_{CTLA, \text{Barr}}$) CTLA-4 molecules outside the synapse is given by:

$$\begin{aligned} T_{CTLA, \text{int}} = & t_{CTLA, \text{tot}}m_{CTLA} - (T_{CTLA, \text{syn}} + C_{CTLA: B72} + C_{CTLA: (B72)2} \\ & + \sum_{k=1}^{\infty} B_k k + \sum_{k=1}^{\infty} C_k(k+1) + \sum_{k=1}^{\infty} E_k k)a_{\text{syn}} - T_{CTLA, \text{Barr}}a_{\text{Barr}} \end{aligned} \quad (4.4)$$

$$\frac{dT_{CTLA, \text{Barr}}}{dt} = \kappa_{\text{Barr}}\frac{T_{CTLA, \text{syn}}a_{\text{syn}}}{a_{\text{Barr}}} - \gamma_{\text{Barr}}T_{CTLA, \text{Barr}}. \quad (4.5)$$

Free molecules within the synapse

Molecules inside the synapse can be both immobile and mobile in the free-diffusion model, and both are assumed to be able to bind ligands. Unbound molecules associate (α) with molecules on the opposing mem-

brane, depleting the pool of unbound molecules inside the synapse, whereas dissociation (δ) releases bound molecules. The unbound mobile surface molecules move in (γ) and out (κ) of the synapse. Intracellular CTLA-4 molecules are injected into the synapse at rate λ . As an example, consider the density of unbound CD28 inside the synapse, which is given by:

$$\begin{aligned} \frac{dT_{CD28, \text{syn}}}{dt} = & -\alpha_1T_{CD28, \text{syn}}D_{B72, \text{syn}} - \alpha_2T_{CD28, \text{syn}}D_{B71, \text{syn}} \\ & - \alpha_{22}T_{CD28, \text{syn}}C_{CD28: B71} + \delta_1C_{CD28: B72} + \delta_2C_{CD28: B71} \\ & + \delta_{22}C_{(CD28)2: B71} + \gamma_{28}\frac{T_{CD28, \text{out}}}{a_{\text{syn}}} - \kappa_{28}f_{CD28}T_{CD28, \text{syn}}. \end{aligned} \quad (5.1)$$

The CD28 molecules inside the synapse associate with either B7-2 at rate α_1 or with B7-1 at the rates α_2 and α_{22} . These complexes dissociate at rates δ_1 , δ_2 , and δ_{22} . Mobile molecules outside the synapse diffuse into the synapse at the rate γ_{28} . Finally, unbound molecules diffuse out of the synapse at rate κ_{28} , whereas immobile molecules will remain inside, as given by the function:

$$f_{CD28} = \frac{(T_{CD28, \text{syn}} + C_{CD28: B71} + 2C_{(CD28)2: B71} + C_{CD28: B72} - i_{CD28})}{(T_{CD28, \text{syn}} + C_{CD28: B71} + 2C_{(CD28)2: B71} + C_{CD28: B72})}. \quad (5.2)$$

Here we assume that the ratio of bound immobile and bound mobile molecules reflects the ratio of total immobile (i_{CD28}) and mobile CD28 molecules within the synapse. The unbound densities of CTLA-4, B7-1, and B7-2 are given by:

$$\begin{aligned} \frac{dT_{CTLA, \text{syn}}}{dt} = & -\alpha_3T_{CTLA, \text{syn}}D_{B72, \text{syn}} - \alpha_4T_{CTLA, \text{syn}}D_{B71, \text{syn}} \\ & - \alpha_{44}\sum_{k=1}^{\infty} T_{CTLA, \text{syn}}E_k - \alpha_{44}\sum_{k=1}^{\infty} T_{CTLA, \text{syn}}B_k + \delta_3C_{CTLA: B72} \\ & + \delta_4E_1 + \delta_{44}\sum_{k=1}^{\infty} C_k + \delta_{44}\sum_{k=1}^{\infty} \frac{E_{k+1}}{2} + \lambda\frac{T_{CTLA, \text{int}}}{a_{\text{syn}}} \\ & + \gamma_{\text{Barr}}\frac{T_{CTLA, \text{Barr}}a_{\text{Barr}}}{a_{\text{syn}}} - \kappa_{\text{Barr}}T_{CTLA, \text{syn}} \end{aligned} \quad (5.3)$$

$$\begin{aligned} \frac{dD_{B71, \text{syn}}}{dt} = & -\alpha_2T_{CD28, \text{syn}}D_{B71, \text{syn}} - \alpha_4T_{CTLA, \text{syn}}D_{B71, \text{syn}} \\ & - \alpha_{44}\sum_{k=1}^{\infty} D_{B71, \text{syn}}E_k - \alpha_{44}\sum_{k=1}^{\infty} D_{B71, \text{syn}}C_k + \delta_2C_{CD28: B71} \\ & + \delta_4E_1 + \delta_{44}\sum_{k=1}^{\infty} B_k + \delta_{44}\sum_{k=1}^{\infty} \frac{E_{k+1}}{2} + \gamma_{\text{DC}}\frac{D_{B71, \text{out}}}{a_{\text{syn}}} \\ & - \kappa_{\text{DC}}f_{B71}D_{B71, \text{syn}} \end{aligned} \quad (5.4)$$

$$\begin{aligned} \frac{dD_{B72, \text{syn}}}{dt} = & -\alpha_1T_{CD28, \text{syn}}D_{B72, \text{syn}} - \alpha_3T_{CTLA, \text{syn}}D_{B72, \text{syn}} \\ & - \alpha_{33}C_{CTLA: B72}D_{B72, \text{syn}} + \delta_1C_{CD28: B72} + \delta_3C_{CTLA: B72} \\ & + \delta_{33}C_{CTLA: (B72)2} + \gamma_{\text{DC}}\frac{D_{B72, \text{out}}}{a_{\text{syn}}} - \kappa_{\text{DC}}f_{B72}D_{B72, \text{syn}}. \end{aligned} \quad (5.5)$$

Results

We first use the free-diffusion model to examine the implications, for interactions in two dimensions (i.e., at the cell surface), of the distinct binding preferences of B7-1 and B7-2 for CD28 and CTLA-4 measured in solution by van der Merwe et al. (29) and Collins et al. (20). We then obtain rigorous expression data, which allow us to simulate physiological complex formation at synapses formed between resting or activated T cells and immature or mature DC, and to study the dependence of the interactions on affinity and expression level, and the effects of deleting B7-1 and B7-2

from the system. Finally, we use the barrier-diffusion/active transport model to compare the effects of membrane organizational differences and receptor transport modes on complex formation.

The binding preferences of B7-1 and B7-2

The stoichiometric and solution reaction-rate data of van der Merwe et al. (29) and Collins et al. (20), and diffusion rates for cell surface molecules derived from the literature (30, 31), were used in simulations in which the proteins were “expressed” in the synapse separately and at equivalent levels (with respect to binding site number) and at equivalent levels (with respect to binding site number), and given 100% mobility. Regardless of receptor valency or expression level, B7-2 always engages more CTLA-4 than CD28, and B7-1 binds more CD28 than does B7-2 (Fig. 2). At the level of individual complexes, therefore, B7-1 is a more effective CD28 ligand than B7-2 in two dimensions, and B7-2 binds CTLA-4 more effectively than it binds CD28.

When each protein is treated as a monovalent species, the ratio of CTLA-4 to CD28 engagement is higher for B7-1 than for B7-2, regardless of expression level, but the differences are modest (<2-fold; Fig. 2A, inset). When B7-1 and CTLA-4 are made bivalent at low levels of expression (i.e., 1000 binding sites/synapse), the ratio of CTLA-4 vs CD28 engagement is 18-fold higher for B7-1 than for B7-2 (Fig. 2B, inset). Because the ratio of CTLA-4 to CD28 receptor engagement by B7-1 or B7-2 will determine the net effectiveness of each protein as inhibitory vs activating ligands when all four proteins are expressed, these observations indicate that, at the synapse, B7-1 is likely to be more inhibitory than B7-2. At higher levels of expression (i.e., 10,000 binding sites/synapse), the ratio of CTLA-4 vs CD28 engagement is lower for B7-1 than for B7-2, due to saturation binding of CTLA-4 by B7-1.

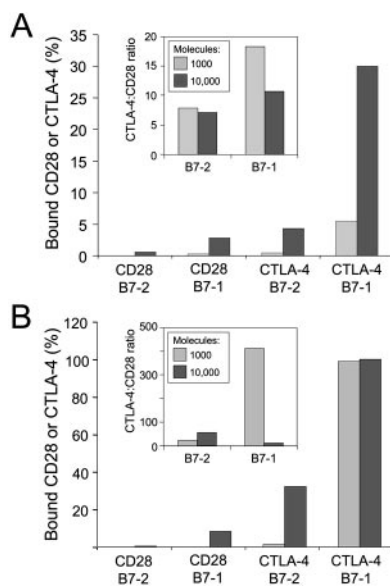


FIGURE 2. Implications of the affinity and stoichiometric differences for interactions at modeled two-dimensional surfaces. Fractions of ligated CD28 and CTLA-4 present at steady state when the molecules are “expressed” separately and at equivalent numbers of binding sites are calculated in simulations based on the free-diffusion model. For each simulation, only the pairs of molecules shown are expressed, at 1000 or 10,000 copies, and all molecules are fully mobile. In *A*, all polypeptides are treated as separate, monovalent binding structures, to examine the effects of the affinity differences only. In *B*, B7-1 and CTLA-4 molecules are allowed to form bivalent structures assumed to be equivalent to their native states. *Insets*, The ratios of CTLA-4 vs CD28 ligation by each ligand (i.e., their CTLA-4 “bias”).

Simulations of complex formation by costimulatory molecules at physiological expression levels

Molecule expression levels. To obtain insights into complex formation at physiological expression levels we undertook a second round of simulations based on rigorous expression data. As far as we can ascertain, quantitative expression data have not previously been obtained for costimulatory molecules. Therefore, we measured the levels of CD28 and CTLA-4 surface expression, and that of B7-1 and B7-2, on resting and PHA-activated ex vivo T cells and immature and polyIC acid-treated mature DCs (iDCs and mDCs), respectively. To do this, we determined the mean fluorescence intensity levels obtained using saturating levels of isotype-matched primary (Fig. 3A) and secondary (Fig. 3B) Abs for each of the Ags relative to that of the TCR (~40,000 per cell; Refs. 5 and 32; cell culture and Ab-staining methods are given in the legend to Fig. 3). The results obtained by gating on the broadest populations are in broad agreement with the striking dichotomy in expression noted in previous qualitative comparisons (Ref. 18; Fig. 3C): whereas CD28 and B7-2 are generally abundant, B7-1 and CTLA-4 are only weakly expressed. CTLA-4 is undetectable on the surface of naive T cells and is up-regulated but still expressed at very low levels on activated T cells. The high expression of CD28 on resting T cells remains essentially unchanged after activation (Fig. 3C). Similar TCR/CD28/CTLA-4 ratios were obtained after gating on T cell subsets (data not shown). For CD28, slightly higher expression was seen on CD4⁺CD45RO⁺ (i.e., memory) cells.

Simulations. Physiological simulations were based initially on the free-diffusion model and the parameters given in Tables III-V. In the absence of well-defined mobilities, we used values of 30% for CD28 (as determined in Ref. 16), and 60% for B7-1 and B7-2 (as obtained for CD2; Ref. 16); CTLA-4 was assigned 100% mobility. Otherwise the molecules were allowed to diffuse freely. Complex formation is simulated in Fig. 4 with, for the sake of simplicity, the emphasis placed on the numbers of complexes formed by CD28 and CTLA-4 at the synaptic interface between pairs of cells in two physiological states: on the one hand, a naive T cell interacting with an iDC or mDC and, on the other, an activated T cell interacting with a mDC. For a naive T cell with a surface area of 113 μm^2 , forming a synapse of $\sim 13 \mu\text{m}^2$ with an iDC, ~ 600 CD28 molecules form complexes with B7 molecules by the time the steady state is reached (Fig. 4A). Their higher expression and faster kinetics lead to the initial accumulation of B7-2/CD28 complexes, but the higher affinity of B7-1 eventually results in the accumulation of almost twice as many B7-1/CD28 complexes. For encounters with a mDC, only 50% more CD28 molecules are engaged (900 in total), suggesting that, in terms of their ability to costimulate naive T cells by ligating CD28, mature and immature DCs are not substantially different.

For the activated T cell interacting with a mDC, the 4-fold increase in the surface area of the activated T cell leads to a 4-fold reduction in the engagement of CD28 (Fig. 4B). CTLA-4 dominates interactions at the synapse when both receptors are expressed, forming more than twice as many complexes as CD28 (Fig. 4C). In the simulations, CTLA-4 is inserted into the synapse during the first 10 min of contact, in accordance with the observations of Egen and Allison (19), whereupon it is immediately and fully ligated. In contrast, only $\sim 2\%$ of the CD28 molecules are complexed with B7-1 or B7-2. CTLA-4 initially forms complexes with B7-2, which are then gradually replaced by B7-1/CTLA-4 complexes. At the steady state, B7-2 engages 33-fold more CD28 than CTLA-4, and B7-1 forms ~ 7 -fold more complexes with

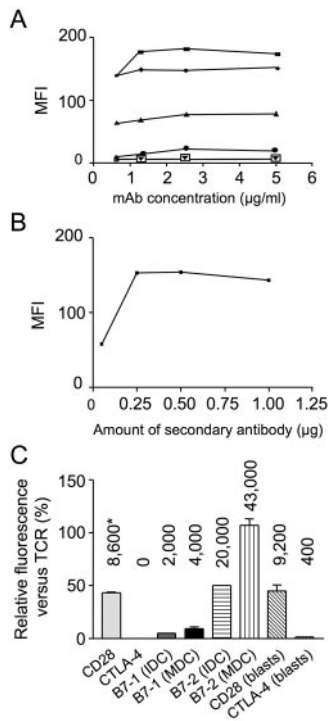


FIGURE 3. Quantitation of costimulatory receptors and ligands on resting and activated T cells, iDCs, and mDCs. *A*, Titration of primary Abs (TCR, squares; CD28, triangles; CTLA-4, inverted triangles; B7-2, diamonds; B7-1, circles; and isotype control, open squares). PBLs were isolated on Lymphoprep gradients and then 5×10^5 cells were stained with the indicated amounts of isotype-matched (IgG1) Abs (anti- $\alpha\beta$ TCR (Serotec); anti-CD28 (BD Biosciences); anti-CTLA-4 (Cambridge Biosciences); anti-B7-1 (Research Diagnostics); anti-B7-2 (BD Biosciences); and isotype control (Serotec)) for 30 min on ice followed by FITC-labeled rat anti-mouse IgG1 Ab (BD Biosciences) at $10 \mu\text{g/ml}$ for a further 30 min. *B*, Titration of the secondary Ab. A total of 5×10^5 PBL were labeled with anti-TCR mAb at $3 \mu\text{g/ml}$ for 30 min and with FITC-labeled rat anti-mouse IgG1 Ab (BD Biosciences) at the indicated concentrations for a further 30 min. *C*, Expression of costimulatory receptors and ligands. PBL were activated with PHA ($50 \mu\text{g/ml}$; Sigma-Aldrich) for 2 days and then stained with saturating levels of the indicated Abs. DCs were derived by *in vitro* maturation of monocytes using GM-CSF (50 ng/ml ; Leucomax, Schering-Plough) and IL-4 (250 IU/L ; Pharmingen) for 6 days. CD14^+ monocytes were initially isolated from human PBMC using positive magnetic bead selection (Miltenyi Biotec). iDCs were then stimulated with polyIC acid ($50 \mu\text{g/ml}$; Sigma-Aldrich) for 48 h. The expression level for each of the surface Ags, shown above each column in the histogram, was based on the ratio of the mean fluorescence index (MFI) for the Ag vs that for the TCR (based on five separate estimates), which was taken to be expressed at 40,000 molecules per cell (5, 32). The expression level for CD28 (*) is adjusted for valency.

CTLA-4 than with CD28. The distribution of size classes for arrays formed by B7-1 and CTLA-4 is shown in Fig. 4*D*. Initially, relatively small arrays are formed, reflecting the early dominance of B7-2, followed by waves of successively larger complex formation. By the time a pseudo steady state is reached ~ 90 min after contact, almost three-quarters of the bound CTLA-4 molecules have formed intermediate-length arrays of 7-18 receptor/ligand pairs each.

Manipulation of the model. In simulations that examined the dependence of the interactions of CD28 and CTLA-4 on affinity (K_a), mobility and expression level (i.e., the number of molecules per cell), each parameter value was reduced 10-fold for all the molecules, and the results compared with those obtained for the acti-

vated T cell/mDC synapse and the default parameter values given in Tables III-V. Reducing the affinities decreases CD28 ligation 7-fold (Fig. 5*A*), whereas CTLA-4 ligation remains largely unchanged (Fig. 5*B*). The interactions of CD28 and CTLA-4 are each highly sensitive to expression levels. Complex formation by CD28 is relatively insensitive to mobility changes, however. The effect of reducing the mobility of CTLA-4 was not tested because, even at the default settings, it is all retained within the synapse. Altering the parameters over a larger range results in qualitatively similar changes in ligation as the 10-fold reduction (data not shown).

In simulations shown in Fig. 4*B*, CTLA-4 exhibits a clear bias toward B7-1 ligation within ~ 30 min. To determine the overall extent to which CTLA-4 ligation is dependent on B7-1, we ran simulations of an *in silico* "knockout" of B7-1. In the absence of B7-1, all the CTLA-4 is rapidly occupied by B7-2 (Fig. 5*C*) and the number of B7-2/CD28 complexes is reduced approximately one-third. Very similar results are obtained when B7-2 is deleted, except that the kinetics of accumulation of both types of complex is substantially reduced (Fig. 5*D*).

Simulations of the effects of membrane barriers and active transport to the synapse. The absence of an obligatory requirement for either B7-1 or B7-2 when a large fraction of the proteins are free to diffuse about the entire surface prompted us to consider additional transport models. The emerging view of the cell surface is that it is divided into corrals bounded by barriers constraining diffusion to mean free path-lengths of the order of $1 \mu\text{m}$ (25), and that all molecules within such corrals are otherwise mobile. We simulated this situation by assuming that the c-SMAC of the synapse forms within one of these corrals, and by allowing all the molecules to be randomly distributed over the entire cell but permitting only those molecules located within the corral, i.e., an area bounded by a barrier $0.5 \mu\text{m}$ from the edge of the synapse, to accumulate within it. This approach for restricting molecules to certain regions of the cell has been implemented by others in the context of TCR/pMHC interactions (6, 33). In the absence of active transport (Fig. 6), $<1\%$ of the total CD28 is engaged, and no complexes form between CD28 and B7-1. Eight-fold more CTLA-4/B7-2 than CTLA-4/B7-1 complexes form, reflecting the low numbers of B7-1 molecules within the synapse. The dominance of B7-2 resulting from its very high expression is exaggerated by active transport (Fig. 6), which we simulated by moving various fractions of the CD28, B7-1, and B7-2 molecules (i.e., 33, 66, and 100%) to the vicinity of the synapse and constraining their diffusion to the area bounded $0.5 \mu\text{m}$ from its edge. With the transport of as few as one-third of the molecules to the synapse, 5-fold more complexes form between B7-2 and CD28 than between B7-1 and CD28. Complex formation by CTLA-4 is less ligand-dependent and all of it is engaged. At the highest levels of active transport, virtually all of the CD28 is ligated and, at the steady state, the ratio of CD28 to CTLA-4 complexes is $>20:1$. Deletion of B7-1 or B7-2 under these conditions is largely without effect, except insofar as less CD28 is engaged when B7-2 is deleted (Fig. 6).

Discussion

The extent to which CD28 and CTLA-4 will express their activating and inhibitory potential at any given time is determined by a complex set of factors involving, in the first instance, the timing and level of coexpression of the two receptors, and the relative strength of their interactions with their shared ligands, B7-1 and B7-2. We have taken an initial step toward unraveling the complexity of this process by constructing a theoretical framework within which it is now possible to directly simulate, rather than qualitatively model, these interactions.

Table V. *Parameter values used in the free-diffusion model (i) and in the barrier-diffusion/active transport model (ii)*

Name	Definition	(i)	(ii)	Units	Ref.
$t_{CD28,tot}$	Total expression of CD28 (naive/activated)	8.6×10^3 9.2×10^3	8.6×10^3 9.2×10^3	Number	— ^a
$t_{CTLA,tot}$	Total expression of CTLA-4 (naive/activated)	0	0	Number	— ^a
$d_{B71,tot}$	Total expression of B7-1 (immature/mature)	0.4×10^3 1×10^3 ^b 2×10^3 ^b	0.4×10^3 1×10^3 ^b 2×10^3 ^b	Number	— ^a
$d_{B72,tot}$	Total expression of B7-2 (immature/mature)	20×10^3 43×10^3	20×10^3 43×10^3	Number	— ^a
m_{CD28}	Mobility of CD28	0.3	1		16
m_{CTLA}	Mobility of CTLA-4	1	1		16
m_{B71}	Mobility of B7-1	0.6	1		16
m_{B72}	Mobility of B7-2	0.6	1		16
i_{CD28}	Immobile CD28 molecules inside synapse (naive/activated)	53 14		Number/ μm^2	— ^c
i_{B71}	Immobile B7-1 molecules inside synapse (immature/mature)	0.32 0.64		Number/ μm^2	— ^c
i_{B72}	Immobile B7-2 molecules inside synapse (immature/mature)	6.37 13.7		Number/ μm^2	— ^c

^a Determined in the present study.

^b It is assumed that the B7-1 molecules are expressed as bivalent dimers.

^c The density of immobile molecules inside the synapse is given by the ratio of the area of the synapse and the total cell surface area, with a given mobility and assuming a random distribution.

This has become possible for two reasons. First, costimulatory molecules represent the only system of interacting activating and inhibitory proteins for which all the binding and structural parameters are now well-characterized. Second, studies of cells interacting with two-dimensional model bilayers (16), along with interference reflection- (14, 34) and electron microscopy-derived data (35), have suggested, notwithstanding the technical limitations of these imaging techniques, that the immunological synapse is a relatively uniform structure favoring costimulatory interactions (16). This meant that we could ignore geometric constraints and thermodynamic parameters related to the initiation of cell-cell contact and adhesion, i.e., we could assume that the opposing membranes had already achieved, and are held at, the optimal distance for the interactions of small signaling proteins. With this assumption, the minimum set of parameters controlling the rates and extent of complex formation, which can be directly simulated using mean-

field ordinary differential equations, consists only of stoichiometric, affinity, diffusion and expression data.

The simulations offer several new insights into the basic properties of the costimulatory system. Imposing barriers upon the membrane, as is required by current models of membrane architecture (25), allows <1% of the CD28 to form complexes, which is likely to be insufficient to account for the visual accumulation observable by fluorescence microscopy (16, 23). This implies that the molecules must be actively transported to the synapse or that the barriers disappear, consistent with the observations of Wulfig and Davis (36) who showed that there is generalized transport of cell surface molecules to the synapse upon activation, a process that is itself enhanced by costimulatory signaling. The simulations show that the transport of just a small fraction of the molecules to the synapse (e.g., one-third; Fig. 6) restores significant levels of engagement when barriers to mobility are present. It does not

FIGURE 4. Complex formation in the free-diffusion model. *A*, Numbers of CD28 molecules bound to B7-1 or B7-2 at the synapse between a naive T cell and an iDC or a mDC. *B*, Numbers of CD28 and CTLA-4 molecules bound to B7-1 or B7-2 at the synapse between an activated T cell and a mDC. *C*, Total numbers of complexed CD28 and CTLA-4 molecules at the synapse between an activated T cell and a mDC. *D*, Numbers of bound CTLA-4 and B7-1 molecules forming multivalent arrays consisting of 1-6, 7-12, 13-18, and >18 bound CTLA-4 molecules. Simulations were run using the parameter values listed in Tables III-V.

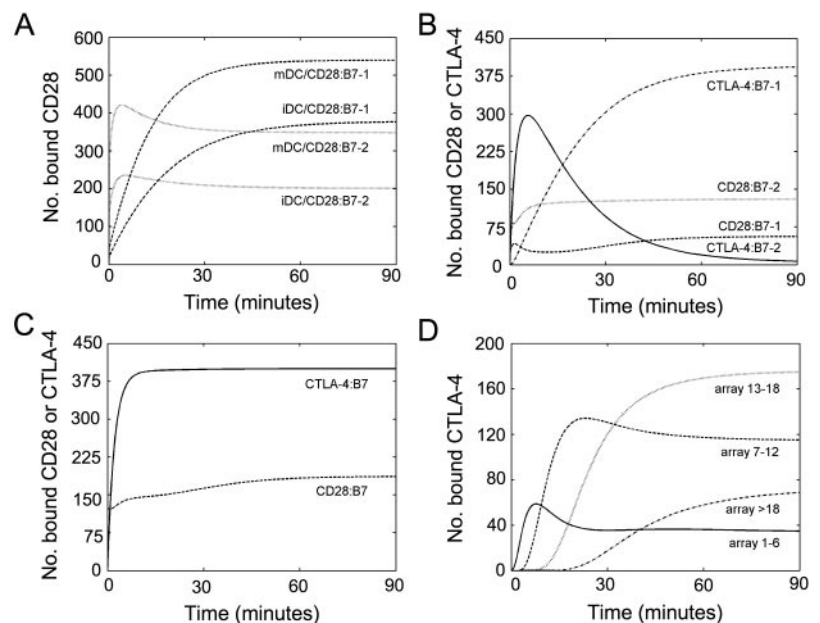
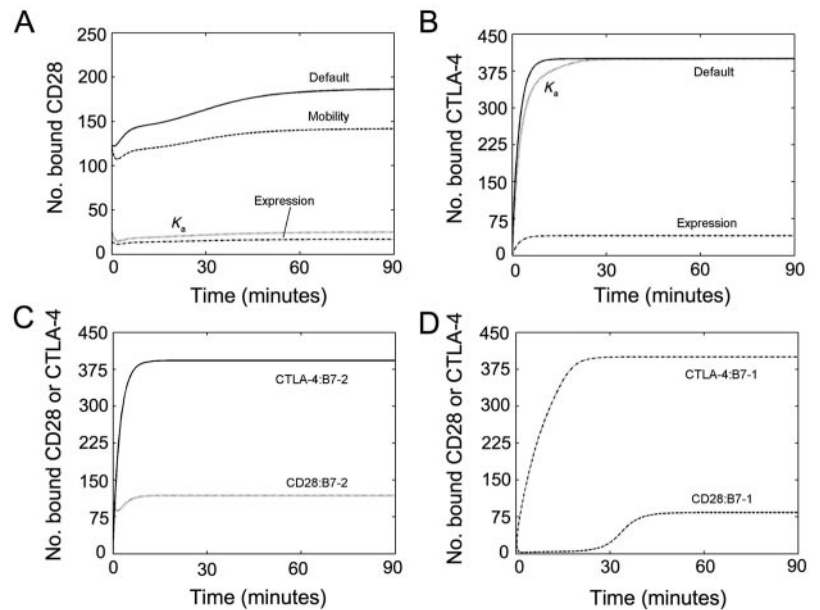


FIGURE 5. The effects of altering parameter values in the free-diffusion model. Numbers of bound (A) CD28 and (B) CTLA-4 at the synapse between an activated T cell and a mDC. The individual parameter values indicated (association constant (K_d), mobility or expression) are reduced 10-fold in the simulations shown, while the remaining parameters (Tables III-V) are kept at default levels. In C, B7-1 is deleted from the simulations ($d_{B71,tot} = 0$) and in D, B7-2 is deleted ($d_{B72,tot} = 0$).



follow that all productive receptor interactions require active transport, however. The high expression and molar excess of the TCR over its ligands, along with the relatively high affinity of their interactions, for example, will ensure that every ligand is engaged within each membrane domain. This in turn allows initiating signals to be triggered in a passive, transport- and signaling-independent manner. Our poor understanding of the quantitative aspects of transport in vivo is the most likely source of uncertainty for the present simulations, given their sensitivity to transport effects.

The simulations imply that complex formation by CD28 is highly dependent on K_d and expression level: reducing the affinities of CD28 for B7-2 and B7-1 10-fold severely reduces complex formation, and a similar reduction in expression completely eliminates it (Fig. 5A). In contrast, the interactions of CTLA-4 are largely insensitive to K_d (Fig. 5B): a 10-fold reduction in K_d still gives complete ligation, indicating that the affinities of CTLA-4 for its ligands are substantially higher than necessary for efficient binding and that CTLA-4 ligation is likely to be tolerant of sub-

stantial variation in the levels of B7-1 and/or B7-2 expression. Dustin et al. (30) have shown that, in two dimensions, the CD48-CD2 interaction (solution $K_d = 70 \mu\text{M}$) is “barely adequate” to sustain binding, suggesting that there is a threshold below which no binding will occur in two dimensions. That the CD28 affinity is apparently close to this limit implies that the level of costimulatory signaling by CD28 could be readily modulated by APCs, simply by varying the levels of expression of the costimulatory ligands, without compromising the inhibitory potential of CTLA-4.

According to our simulations, the interactions of CD28 and CTLA-4 with their ligands are likely to be highly dynamic during the early stages of contact between an activated T cell and a mDC (i.e., < 30 min). B7-2 is the dominant ligand for both CD28 and CTLA-4 for the first 15 min due to its higher expression levels. The much greater affinity of B7-1 for CTLA-4, however, leads eventually to the complete replacement of B7-2 by B7-1, although the overall level of CTLA-4 ligation remains largely unchanged. More CTLA-4 than CD28 complexes form within a minute of contact due to the high affinity of CTLA-4 for B7-1 and B7-2, indicating that CTLA-4 is likely always to be dominant when the receptors are coexpressed, and that synapses formed when CTLA-4 is present may invariably be inhibitory (Fig. 4, B and C). The presence of CTLA-4 reduces CD28 complex formation by a factor of two supporting the proposal that the inhibitory effects of CTLA-4 involve, at least in part, competition for ligands between CD28 and CTLA-4 (reviewed in Ref. 37). Moreover, given that 2-fold more CTLA-4 than CD28 complexes assemble at the synapse, it is unnecessary to postulate that the signals generated per complex by CTLA-4 are intrinsically more potent than those invoked by CD28 to account for the observation (38) that CTLA-4 signaling is dominant over that by CD28.

An important goal of the present study was to understand the likely implications of stoichiometric and affinity differences measured in solution (e.g., Ref. 20) for protein interactions occurring at synapses. A general point we can now make is that stoichiometric properties, expression levels and, for receptors that share ligands, competition effects are likely to profoundly influence complex formation at cellular interfaces. This is illustrated by the effects of these factors on the CTLA-4:CD28 engagement ratio, or “CTLA-4 bias”, of each ligand. The B7-1 bias is 18-fold higher than that of B7-2 when the proteins are expressed at equivalent

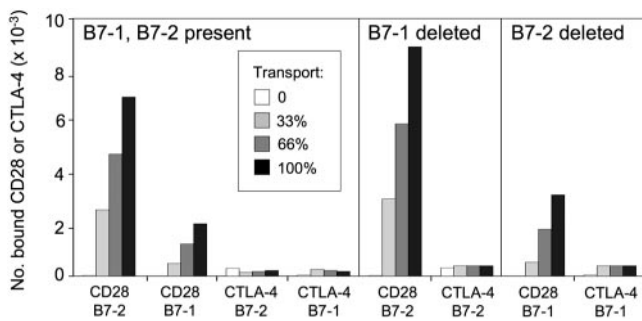


FIGURE 6. The numbers of bound CD28 and CTLA-4 molecules at the synapse between an activated T cell and a mDC at steady state, simulated using the barrier-diffusion/active transport model. The simulation is initiated after placing 0, 33, 66, or 100% of the CD28, B7-1 and B7-2 molecules that would otherwise be distributed outside the corral, within the area bounded by a barrier $0.5 \mu\text{m}$ from the synapse. Simulations were done with parameter values listed in Tables III-V, with the exception of the simulations in which B7-1 ($d_{B71,tot} = 0$) or B7-2 ($d_{B72,tot} = 0$) are deleted. Note that, for some of the simulations run with zero transport, the numbers of complexes formed are too low to be visible in the histograms.

levels at the synapse and CTLA-4 and B7-1 are allowed to interact bivalently (Fig. 2B). For monovalent forms of the proteins, the difference in bias is only 2-fold (Fig. 2A), which is comparable to the ~2.5-fold difference in the CTLA-4:CD28 affinity ratios measured in solution (20), emphasizing the importance of valency effects. Allowing for competition under these conditions, the B7-1 bias is 2750-fold higher than that of B7-2 (data not shown). Taking into account the actual levels of expression reduces this difference to 231-fold (Fig. 4B). The net effect is that in the simulations of physiological interactions the receptor binding preferences polarize: B7-2 engages 33-fold more CD28 than CTLA-4 molecules, whereas B7-1 forms ~7-fold more complexes with CTLA-4 than with CD28. Virtually all the CTLA-4 is engaged by B7-1 only, forming linear arrays of 7-18 complexes.

These observations are in excellent agreement with the predictions of Collins et al. (20), and the conclusions of Pentcheva-Hoang et al. (23), i.e., that B7-2 and B7-1 are not interchangeable and are instead the dominant ligands of CD28 and CTLA-4, respectively. Our findings differ from those of Pentcheva-Hoang et al. (23) only when B7-1 is deleted from the system. Using B7-1- and B7-2-deficient APCs, Pentcheva-Hoang et al. (23) showed that B7-2 is incapable of recruiting CTLA-4 to the synapse and that CD28 is apparently only recruited by B7-2, and argued that this is a direct consequence of the distinct binding properties of B7-2 and B7-1 reported by Collins et al. (20). The simulations have allowed a direct test of this proposal because they depend only on the binding, expression, and diffusion/transport properties of the molecules and B7-1 can easily be deleted from the equations. Regardless of whether the molecules freely diffuse to the synapse or are actively transported there, the simulations show that CTLA-4 is fully ligated by B7-2 in the absence of B7-1 (Figs. 5 and 6); according to the free-diffusion model, B7-2 recruits ~3-fold more CTLA-4 than CD28 (Fig. 5). By altering the affinities it is possible to mimic the observations of Pentcheva-Hoang et al. (23) in our simulations. To prevent CTLA-4 accumulation by B7-2 in the absence of B7-1, however, to the extent that the ratio of CD28:CTLA-4 complexes is 10:1 for example, it is necessary to reduce the B7-2/CTLA-4 affinity 240-fold (data not shown). How can these observations be reconciled? Assuming that the measurements of Collins et al. (20) are not in error by more than two orders of magnitude, the ability of B7-1 but not B7-2 to visibly recruit CTLA-4 (23) suggests that the mechanism of its accumulation is not ligand binding-dependent only. One possibility is that the activating signals generated by B7-1 are much better at inducing CTLA-4 expression than those invoked by B7-2. In the case of B7-2 deletion, the apparent nonaccumulation of CD28 by B7-1 (23) is likely to reflect the difficulty in detecting the small number of B7-1-engaged receptors against a large background of unengaged CD28 molecules (e.g., 80 complexes vs 8520 uncomplexed CD28 molecules in the simulation shown in Fig. 5D). A scenario consistent with both the present analysis and the data of Pentcheva-Hoang et al. (23) is that early signaling by CD28/B7-2 complexes is relatively weak and that the subsequent, elevated expression of B7-1 allows more potent CD28 signaling that enhances CTLA-4 expression, reinforcing inhibition of the response.

It is surprising that there appears to be no absolute requirement for B7-1 as a ligand for CD28 or CTLA-4, given our starting assumptions. Interactions involving B7-1 are enigmatic insofar as they could be as much as 10,000–1,000,000 times more stable than TCR/pMHC or B7-2/CD28 interactions (20). The very large excess of B7-2 over CD28 and CTLA-4, however, ensures the ligation of these molecules in the absence of B7-1 in our simulations. So why is B7-1 there at all? Two types of explanation are feasible. First, the principal role of B7-1 might not involve inhibitory sig-

naling to T cells late in immune responses. It has been proposed that the interactions of B7-1 expressed on iDCs play an important role in maintaining self-tolerance by engaging CTLA-4 expressed constitutively on regulatory T cells (reviewed in Ref. 37). For cells constitutively expressing CTLA-4, rather than inserting it directly into the synapse, it is possible that only B7-1 is capable of forming sufficient numbers of regulatory complexes. This can be tested in our simulations when the levels of expression of these molecules on regulatory T cells have been determined. The interactions of CD28 and CTLA-4 with B7-1 and B7-2 are now also thought to have “reverse” signaling effects on DCs (39, 40) and it is highly likely that the nature of the signals are distinct given the sequence differences in the cytoplasmic domains of B7-1 and B7-2, and differences in the strength and valency of their interactions with CD28 and CTLA-4. Alternatively, the observations of Pentcheva-Hoang et al. (23) imply that the binding of B7-1 to CD28 could be more important than its interaction with CTLA-4. The extended half-lives of B7-1/CD28 vs B7-2/CD28 complexes may enhance CTLA-4 expression via a kinetic proofreading-based mechanism; thereafter, it may not matter which ligand engages CTLA-4. A second possibility we have to consider is that our starting assumptions are oversimplistic and that conditions within the synapse are more complex than we think. The simulations show that CTLA-4 initially forms mostly bivalent complexes with B7-2, and that these convert to multivalent complexes with B7-1 at a later stage. Studies using transfected ligands suggest that B7-2/CTLA-4 interactions are not inhibitory (41). Other work suggests that the synapse could be less geometrically uniform than is generally believed: for synapses formed by NK cells, the size of the synaptic “cleft” varies up to 50 nm, and large molecules such as CD43 are not always excluded (42). In a more dynamic synaptic microenvironment, the multivalent arrays that only B7-1 can form, or their intrinsically higher affinity, or both, may ensure that CTLA-4 is efficiently and stably ligated.

Acknowledgments

We are grateful to Ed Evans, Anton van der Merwe, and David Sansom for helpful comments on the manuscript.

Disclosures

The authors have no financial conflict of interest.

References

- Chakraborty, A. K., M. L. Dustin, and A. S. Shaw. 2003. In silico models for cellular and molecular immunology: successes, promises and challenges. *Nat. Immunol.* 4: 933–936.
- Goldstein, B., J. R. Faeder, and W. S. Hlavacek. 2004. Mathematical and computational models of immune-receptor signalling. *Nat. Rev. Immunol.* 4: 445–456.
- McKeithan, T. W. 1995. Kinetic proofreading in T-cell receptor signal transduction. *Proc. Natl. Acad. Sci. USA* 92: 5042–5046.
- Hlavacek, W. S., A. Redondo, H. Metzger, C. Wofsy, and B. Goldstein. 2001. Kinetic proofreading models for cell signaling predict ways to escape kinetic proofreading. *Proc. Natl. Acad. Sci. USA* 98: 7295–7300.
- Valitutti, S., S. Muller, M. Cella, E. Padovan, and A. Lanzavecchia. 1995. Serial triggering of many T-cell receptors by a few peptide-MHC complexes. *Nature* 375: 148–151.
- Wofsy, C., D. Coombs, and B. Goldstein. 2001. Calculations show substantial serial engagement of T cell receptors. *Biophys. J.* 80: 606–612.
- Qi, S. Y., J. T. Groves, and A. K. Chakraborty. 2001. Synaptic pattern formation during cellular recognition. *Proc. Natl. Acad. Sci. USA* 98: 6548–6553.
- Burroughs, N. J., and C. Wulfig. 2002. Differential segregation in a cell-cell contact interface: the dynamics of the immunological synapse. *Biophys. J.* 83: 1784–1796.
- Lee, S. J., Y. Hori, J. T. Groves, M. L. Dustin, and A. K. Chakraborty. 2002. The synapse assembly model. *Trends Immunol.* 23: 500–504.
- Lee, S. J., Y. Hori, J. T. Groves, M. L. Dustin, and A. K. Chakraborty. 2002. Correlation of a dynamic model for immunological synapse formation with effector functions: two pathways to synapse formation. *Trends Immunol.* 23: 492–499.

11. Coombs, D., M. Dembo, C. Wofsy, and B. Goldstein. 2004. Equilibrium thermodynamics of cell-cell adhesion mediated by multiple ligand-receptor pairs. *Biophys. J.* 86: 1408–1423.
12. Lee, K. H., A. R. Dinner, C. Tu, G. Campi, S. Raychaudhuri, R. Varma, T. N. Sims, W. R. Burack, H. Wu, J. Wang, et al. 2003. The immunological synapse balances T cell receptor signaling and degradation. *Science* 302: 1218–1222.
13. Monks, C. R., B. A. Freiberg, H. Kupfer, N. Sciaky, and A. Kupfer. 1998. Three-dimensional segregation of supramolecular activation clusters in T cells. *Nature* 395: 82–86.
14. Grakoui, A., S. K. Bromley, C. Sumen, M. M. Davis, A. S. Shaw, P. M. Allen, and M. L. Dustin. 1999. The immunological synapse: a molecular machine controlling T cell activation. *Science* 285: 221–227.
15. Davis, M. M., M. Krosgaard, J. B. Huppa, C. Sumen, M. A. Purbhoo, D. J. Irvine, L. C. Wu, and L. Ehrlich. 2003. Dynamics of cell surface molecules during T cell recognition. *Annu. Rev. Biochem.* 72: 717–742.
16. Bromley, S. K., A. Iaboni, S. J. Davis, A. Whitty, J. M. Green, A. S. Shaw, A. Weiss, and M. L. Dustin. 2001. The immunological synapse and CD28-CD80 interactions. *Nat. Immunol.* 2: 1159–1166.
17. Davis, S. J., S. Ikemizu, E. J. Evans, L. Fugger, T. R. Bakker, and P. A. van der Merwe. 2003. The nature of molecular recognition by T cells. *Nat. Immunol.* 4: 217–224.
18. Lenschow, D. J., T. L. Walunas, and J. A. Bluestone. 1996. CD28/B7 system of T cell costimulation. *Annu. Rev. Immunol.* 14: 233–258.
19. Egen, J. G., and J. P. Allison. 2002. Cytotoxic T lymphocyte antigen-4 accumulation in the immunological synapse is regulated by TCR signal strength. *Immunity* 16: 23–35.
20. Collins, A. V., D. W. Brodie, R. J. Gilbert, A. Iaboni, R. Manso-Sancho, B. Walse, D. I. Stuart, P. A. van der Merwe, and S. J. Davis. 2002. The interaction properties of costimulatory molecules revisited. *Immunity* 17: 201–210.
21. Ikemizu, S., R. J. Gilbert, J. A. Fennelly, A. V. Collins, K. Harlos, E. Y. Jones, D. I. Stuart, and S. J. Davis. 2000. Structure and dimerization of a soluble form of B7-1. *Immunity* 12: 51–60.
22. Stamper, C. C., Y. Zhang, J. F. Tobin, D. V. Erbe, S. Ikemizu, S. J. Davis, M. L. Stahl, J. Seehra, W. S. Somers, and L. Mosyak. 2001. Crystal structure of the B7-1/CTLA-4 complex that inhibits human immune responses. *Nature* 410: 608–611.
23. Pentcheva-Hoang, T., J. G. Egen, K. Wojnoonski, and J. P. Allison. 2004. B7-1 and B7-2 selectively recruit CTLA-4 and CD28 to the immunological synapse. *Immunity* 21: 401–413.
24. Agrawal, N. G., and J. J. Linderman. 1996. Mathematical modeling of helper T lymphocyte/antigen-presenting cell interactions: analysis of methods for modifying antigen processing and presentation. *J. Theor. Biol.* 182: 487–504.
25. Vereb, G., J. Szollosi, J. Matko, P. Nagy, T. Farkas, L. Vigh, L. Matyus, T. A. Waldmann, and S. Damjanovich. 2003. Dynamic, yet structured: The cell membrane three decades after the Singer-Nicolson model. *Proc. Natl. Acad. Sci. USA* 100: 8053–8058.
26. Szabo, A., K. Schulten, and Z. Schulten. 1980. First passage time approach to diffusion controlled reactions. *J. Chem. Phys.* 72: 4350–4357.
27. Bell, G. I. 1978. Models for the specific adhesion of cells to cells. *Science* 200: 618–627.
28. Linsley, P. S., J. Bradshaw, J. Greene, R. Peach, K. L. Bennett, and R. S. Mittler. 1996. Intracellular trafficking of CTLA-4 and focal localization towards sites of TCR engagement. *Immunity* 4: 535–543.
29. van der Merwe, P. A., D. L. Bodian, S. Daenke, P. Linsley, and S. J. Davis. 1997. CD80 (B7-1) binds both CD28 and CTLA-4 with a low affinity and very fast kinetics. *J. Exp. Med.* 185: 393–403.
30. Dustin, M. L., D. E. Golan, D. M. Zhu, J. M. Miller, W. Meier, E. A. Davies, and P. A. van der Merwe. 1997. Low affinity interaction of human or rat T cell adhesion molecule CD2 with its ligand aligns adhering membranes to achieve high physiological affinity. *J. Biol. Chem.* 272: 30889–30898.
31. Favier, B., N. J. Burroughs, L. Wedderburn, and S. Valitutti. 2001. TCR dynamics on the surface of living T cells. *Int. Immunol.* 13: 1525–1532.
32. Labrecque, N., L. S. Whitfield, R. Obst, C. Waltzinger, C. Benoist, and D. Mathis. 2001. How much TCR does a T cell need? *Immunity* 15: 71–82.
33. Coombs, D., A. M. Kalergis, S. G. Nathanson, C. Wofsy, and B. Goldstein. 2002. Activated TCRs remain marked for internalization after dissociation from pMHC. *Nat. Immunol.* 3: 926–931.
34. Dustin, M. L., L. M. Ferguson, P. Y. Chan, T. A. Springer, and D. E. Golan. 1996. Visualization of CD2 interaction with LFA-3 and determination of the two-dimensional dissociation constant for adhesion receptors in a contact area. *J. Cell Biol.* 132: 465–474.
35. Donnadieu, E., P. Revy, and A. Trautmann. 2001. Imaging T-cell antigen recognition and comparing immunological and neuronal synapses. *Immunology* 103: 417–425.
36. Wulfig, C., and M. M. Davis. 1998. A receptor/cytoskeletal movement triggered by costimulation during T cell activation. *Science* 282: 2266–2269.
37. Sansom, D. M., C. N. Manzotti, and Y. Zheng. 2003. What's the difference between CD80 and CD86? *Trends Immunol.* 24: 314–319.
38. Mandelbrot, D. A., A. J. McAdam, and A. H. Sharpe. 1999. B7-1 or B7-2 is required to produce the lymphoproliferative phenotype in mice lacking cytotoxic T lymphocyte-associated antigen 4 (CTLA-4). *J. Exp. Med.* 189: 435–440.
39. Orabona, C., U. Grohmann, M. L. Belladonna, F. Fallarino, C. Vacca, R. Bianchi, S. Bozza, C. Volpi, B. L. Salomon, M. C. Fioretti, et al. 2004. CD28 induces immunostimulatory signals in dendritic cells via CD80 and CD86. *Nat. Immunol.* 5: 1134–1142.
40. Fallarino, F., U. Grohmann, K. W. Hwang, C. Orabona, C. Vacca, R. Bianchi, M. L. Belladonna, M. C. Fioretti, M. L. Alegre, and P. Puccetti. 2003. Modulation of tryptophan catabolism by regulatory T cells. *Nat. Immunol.* 4: 1206–1212.
41. Manzotti, C. N., H. Tipping, L. C. Perry, K. I. Mead, P. J. Blair, Y. Zheng, and D. M. Sansom. 2002. Inhibition of human T cell proliferation by CTLA-4 utilizes CD80 and requires CD25⁺ regulatory T cells. *Eur. J. Immunol.* 32: 2888–2896.
42. McCann, F. E., B. Vanherberghen, K. Eleme, L. M. Carlin, R. J. Newsam, D. Goulding, and D. M. Davis. 2003. The size of the synaptic cleft and distinct distributions of filamentous actin, ezrin, CD43, and CD45 at activating and inhibitory human NK cell immune synapses. *J. Immunol.* 170: 2862–2870.
43. Abbas, A. K., A. H. Lichtman, and J. S. Pober. 1997. In *Cellular And Molecular Immunology*, 3rd Ed. W. B. Saunders, Philadelphia.
44. Goldsby, R. A., T. J. Kindt, and B. A. Osborne. 2000. In *Kuby Immunology*, 4th Ed. W. H. Freeman, New York.
45. Yanagawa, Y., and K. Onoe. 2002. CCL19 induces rapid dendritic extension of murine dendritic cells. *Blood* 100: 1948–1956.